



THE NATURE AND EFFECT OF SULPHUR COMPOUNDS ON CO₂ AND AIR REACTIVITY OF PETROL COKE

Yaw Delali Bensah¹ and Trygve Foosnaes²

¹Department of Materials Science and Engineering, University of Ghana, Accra-Ghana

²Department of Materials Science and Engineering, Norwegian University of Science and Technology, Trondheim-Norway

E-Mail: bensahyad@yahoo.co.uk

ABSTRACT

Three different single-source coke types (SSA, SSB and SSC) were studied for their air and CO₂ reactivities using the Hydro method and the observed correlation with reactivity determinant parameter such as elemental composition was noted. The reaction temperatures were 525 °C and 960 °C for air and CO₂ reactivities, respectively. Coke sample SSA recorded the highest CO₂ reactivity value of 166 mg/g h while coke sample SSB recorded the lowest value of 25 mg/g h. The coke CO₂ reactivity showed a moderately strong correlation with the combined effect of Na, Fe and Ca concentrations. The inhibitory effect of sulphur as a catalytic poison on Na was observed with significant downward trend in CO₂ reactivity of the investigated cokes. Coke air reactivities showed the expected strong correlation with V. Air reactivity was highest in sample SSC (262 mg/g h) at V concentration of 378 ppm and lowest in sample SSB (39.6 mg/g h) at V concentration of 68 ppm. Sample SSA recorded reactivity value of 129.6 mg/g h at V concentration of 147 ppm. The compound 1-butanethiol was identified by 1-D ¹H NMR and ¹³C NMR, and by 2-D COSY, HSQC and HMBC NMR spectroscopic techniques. It is proposed that 1-butanethiol is one of the possible organosulphur compounds responsible for the reaction with Na forming a stable non-mobile complex partially inhibiting the catalytic effect of Na.

Keywords: petrol coke, reactivity, organosulphur compounds.

INTRODUCTION

Anode quality has one of the largest variable impacts on the aluminium smelting cost with the raw materials strongly influencing the cell operation parameters. The goal of many anode manufacturers is to process the materials for optimum properties in order to meet the anode requirements of aluminium smelters [1]. However, the susceptibility of petroleum coke to airburn and CO₂ attack (measured and reported as air and CO₂ reactivities, respectively) are influenced by the feed material used in the petroleum refining and the coke processing during delayed coking which are determined by two basic parameters; purity and structure [2]. Poor anode quality leads to a decline of cell operation parameters such as current efficiency, consumption of energy, anodes and fluorides, metal quality, amount of work involved etc. [3]. Impurities from the crude oil such as metals and sulphur tend to be concentrated in the heavy residue and hence in the petroleum coke [4]. Reports [5] show that anode carbon can become second to alumina costs as the most important expenditure in aluminium production. Studies show that anode costs account for about 20 % of the total cost of aluminium production, and so reducing anode consumption can have an important impact on a smelter's profitability [6].

Air and CO₂ reactivities have been characterized to be the determinant of the greater part of the excess carbon consumption per tonne of aluminium produced. It is known that excess consumption arises mainly from either direct oxidation of the anode by oxygen or oxidation of the anode by CO₂ which occurs in the pores of the anode or on the grains of carbon dust floating in the bath of the aluminium electrolytic cell. Monitoring the anode

consumption represents an area in which significant cost reductions can be made [7].

In this respect producers of prebaked anodes for aluminium electrolysis are continually seeking to improve anode quality in order to reduce aluminium production costs [8]. Quantifying coke reactivity can be used to correlate values of anode reactivity data. If reliable correlations exist, then CO₂ and air reactivities may be used in predicting anode reactivity [9]. This can be useful in selecting raw materials for the manufacture of commercial anodes with a potential of high resistance to reactivities of CO₂ and air.

On the other hand, during calcining of high sulphur coke, compounds of sulphur are driven off and condense in the coke pores and on the surface. These compounds become active when making anodes of high Na concentration. These sulphur compounds are readily available to Na⁺ to form sulphide or sulphate compounds during anode baking, partly inhibiting the detrimental effect of Na⁺ as an oxidation catalyst [10]. It is probable that sulphur acts as a gasification inhibitor in such reactions since the element can form very stable metal sulphide compounds and is known to be a potent metal catalyst poison [11]. It is postulated that the inhibitive effect of sulphur on the Na catalyzed CO₂ gasification of anodes is caused by the formation of a stable non-mobile Na-S-O complex that prevents Na from catalyzing the reaction at the active sites [12]. Knowledge of the nature of these sulphur compounds can improve the understanding of the mechanism and the inhibition effect on CO₂ reactivity.

In this work air and CO₂ reactivities of carbon samples were studied by the Hydro method. In addition studies were carried out on the extraction and structural



identification of the organosulphur compounds from the coke samples that react with Na^+ , forming stable inactive species inhibiting the catalysis of CO_2 gasification reaction. NMR spectroscopic techniques were used for the structural identification of the organosulphur compounds. The elemental composition of the three coke samples were determined by X-ray Fluorescence method whiles the number of compounds found in the extracts of the coke samples were determined by thin layer chromatography (TLC).

MATERIALS AND METHODS

Materials

The chemicals used in this study were nitrogen, 99.999 %; oxygen, 99.999 %; carbon dioxide, 99.95 % (all from AGA AS, Oslo-Norway); acetone, 99.8 % (Labskan

Ltd, Dublin-Ireland); ethanol, 96 % (Arcus A.S, Oslo - Norway); ethyl acetate, 100 %; n-hexane, 97 % (all from BDH Chemicals Ltd, Poole-England); CDCl_3 , 99.8 % (Sigma-Aldrich, Missouri-U.S.A); Al TLC silica gel 60 F254 (Merck KGaA, Darmstadt Germany). Single source crude calcined cokes A, B and C (SSA, SSB and SSC) were used for the reactivity tests.

Experimental procedure for CO_2 and air reactivities

The CO_2 and air reactivity tests were carried out using the Hydro method as shown diagrammatically in Figure-1. The sample particle sizes (x) for the reactivity measurements fell in the range $150 < x > 250 \mu\text{m}$ and these were maintained in all the experiments for the three coke types. For both CO_2 and air reactivities, five parallel experiments were run for each coke type (SSA, SSB and SSC).

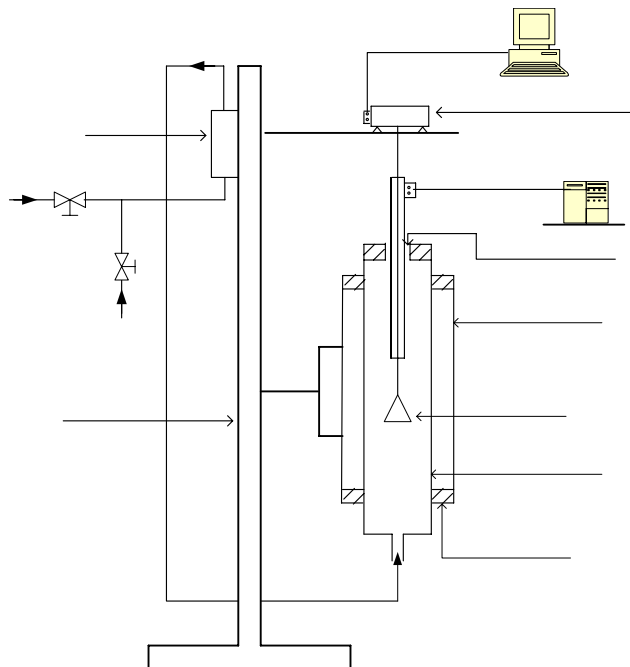


Figure-1. Schematic representation of the experimental setup.

Figure-1 is the schematic representation of the experimental setup. The experiments were carried out under isothermal conditions. The furnace type employed was a gold-coated quartz tube-furnace. The lower part of the sample holder acted as the control thermocouple. The recorder (personal computer) connected to the balance continuously recorded mass changes for every 10 seconds to the nearest of 0.001 g. In the actual experiment coke sample of 1 g was transferred to the sample holder. For the CO_2 reactivity experiments the furnace was heated and kept at $960 \pm 1^\circ\text{C}$. Simultaneously, the furnace was purged with nitrogen (N_2) gas at a constant flow rate of 1.5 l/min until a stable temperature and mass of the sample were observed. The N_2 flowing to the furnace was switched off and CO_2 admitted into the furnace at the same flow rate to start the reaction. The weight of the sample was automatically recorded every 10 seconds for 3 hours after

which the gas was switched back to N_2 . The recorder displayed a linear weight change against time. The same procedure was repeated for air reactivity using air as the reaction gas at a temperature of 525°C .

Experimental procedure for spectroscopic and chromatographic analyses

The extraction of the adsorbed sulphur compounds, the coke samples of particle sizes $104 < x > 250 \mu\text{m}$ (SSA, SSB and SSC) were weighed into batches of 100 g each. A given batch was refluxed with acetone for 8 hours using a Soxhlet apparatus.

For nuclear magnetic resonance (NMR) analysis the sample extracts obtained above from the three coke samples were evaporated to dryness. The resulting solids were dissolved in 1 ml deuterated chloroform (CDCl_3). The samples were transferred into 5 mm diameter NMR



tubes to a height of 5 cm. Spectra for ^1H NMR, ^{13}C NMR and 2-D NMR were obtained from 300 and 400 MHz (DPX300 and DPX400 Avanc Bruker) NMR spectrometers.

The one dimensional (1-D) proton NMR (^1H) and ^{13}C NMR signals (Figures 3 and 4) obtained were difficult to interpret due to their complex spectra resulting from the mixture of compounds where the spectra have many coincident resonances (overlap). These difficulties were circumvented by employing two dimensional (2-D) NMR procedures which were used in the interpretation. Information obtained from 2-D data was used to derive firm conclusions about connectivities between ^1H - ^1H , ^1H - ^{13}C , ^{13}C - ^{13}C subunits. The 2-D techniques used were Correlation Spectroscopy (^1H - ^1H COSY), Heteronuclear Multiple Bond Correlation (HMBC) and Heteronuclear Single Quantum Correlation (HSQC) [13]. For the thin layer chromatographic analyses, the stationary phase was

200 μm thick, 5×10 cm silica-gel- coated aluminium plate and the mobile phase was a 1:1 mixture of ethyl acetate and n-hexane. The separated components of the samples were observed and counted under room and ultraviolet light. The elemental compositions of the petrol cokes were determined using XRF.

RESULTS

In order to determine the reactivities the exposure times to CO_2 and air were noted. Plots of weight loss against time were made. The reactivities (R) were computed from the slope of the linear regression plot from the last half (1.5 hours) because during this period the system is stabilized for both CO_2 and air reactivities for all the five parallel experiments for samples SSA, SSB and SSC. Using the graphical plot of experiment one of sample SSA as a representative plot shown in Figure-2, the reactivities were computed from equations 1, 2 and 3.

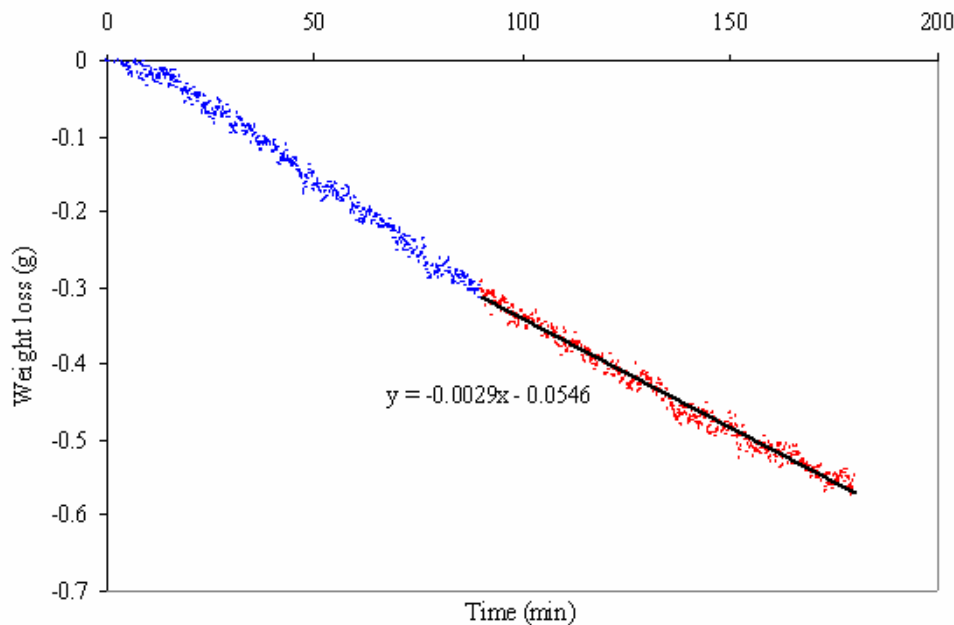


Figure-2. Weight loss as a function of time for experiment SSA1.

$$\Delta W = a \cdot t + b \quad (1)$$

$$R = \frac{(a \cdot 1000 \cdot 60)}{m_i} \quad (2)$$

$$R = \frac{(a \cdot 1000 \cdot 60)}{A} \quad (3)$$

Where ΔW , a , m_i , t and b are the weight loss (g), a constant (gradient), the initial mass of sample (g), time (min) and intercept respectively.

**Table-1.** Reactivity values determined for sample SSA.

Expts	R with CO ₂		R with air	
	mg/gh	mg/cm ² h	mg/gh	mg/cm ² h
SSA1	174	45.8	132	34.7
SSA2	162	42.6	126	33.1
SSA3	168	44.2	132	34.7
SSA4	180	47.3	126	33.1
SSA5	150	39.4	132	34.7
Mean	166.8	43.9	129.6	34.1
Std dev	10.3	2.7	2.9	0.8

Table-2. Reactivity values determined for sample SSB.

Expts	R with CO ₂		R with air	
	mg/gh	mg/cm ² h	mg/gh	mg/cm ² h
SSB1	24	6.3	42	11
SSB2	24	6.3	42	11
SSB3	30	7.9	36	9.5
SSB4	30	7.9	42	11
SSB5	18	4.7	36	9.5
Mean	25.2	6.6	39.6	10.4
Std dev	4.5	1.2	2.9	0.4

Table-3. Reactivity values determined for sample SSC.

Expts	R with CO ₂		R with air	
	mg/gh	mg/cm ² h	mg/gh	mg/cm ² h
SSC1	84	22.1	264	69.4
SSC2	84	22.1	256	67.3
SSC3	72	18.9	276	72.6
SSC4	96	25.2	252	66.3
SSC5	84	22.1	264	69.4
Mean	84	22.1	262.4	69
Std dev	7.6	2	8.2	2.2

Table-4. The elemental composition of samples.

Element	Na	Mg	Al	Si	S (%)	K	Ca	Ti	V	Mn	Fe	Ni	Zn
SSA (ppm)	55	12	54	63	1.2	3	110	3	147	4	105	82	2
SSB (ppm)	28	4	61	105	1	6	42	3	68	4	189	44	4
SSC (ppm)	43	8	24	23	2.6	2	27	1	378	1	378	170	2

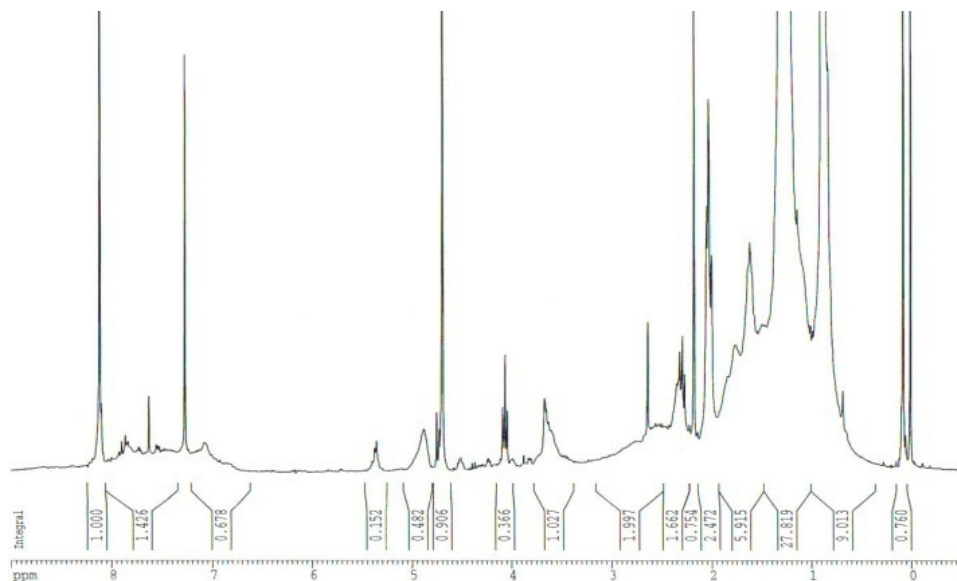


Figure-3. Proton (^1H) NMR spectrum of sample SSA in CDCl_3 run at 300 MHz.

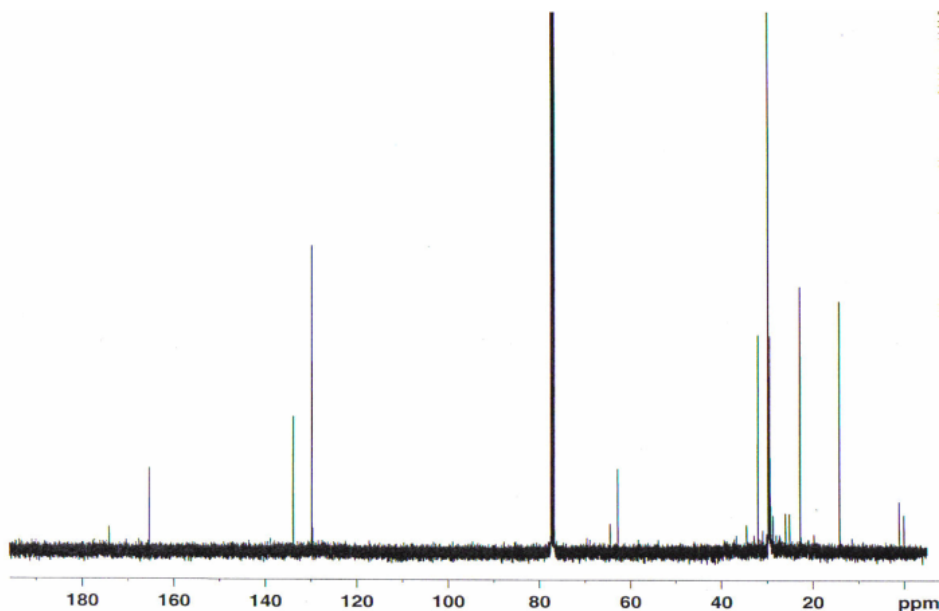


Figure-4. Carbon (^{13}C) NMR spectrum of sample SSA in CDCl_3 run at 300 MHz.

As obtained in Figure-5, the COSY spectrum shows a correlation between directly coupled protons, i.e. interactions between protons on adjacent carbons. The

diagonal and the projection on each axis show the one dimensional spectrum. The off-diagonal peaks indicate the presence of coupling between pairs of protons.

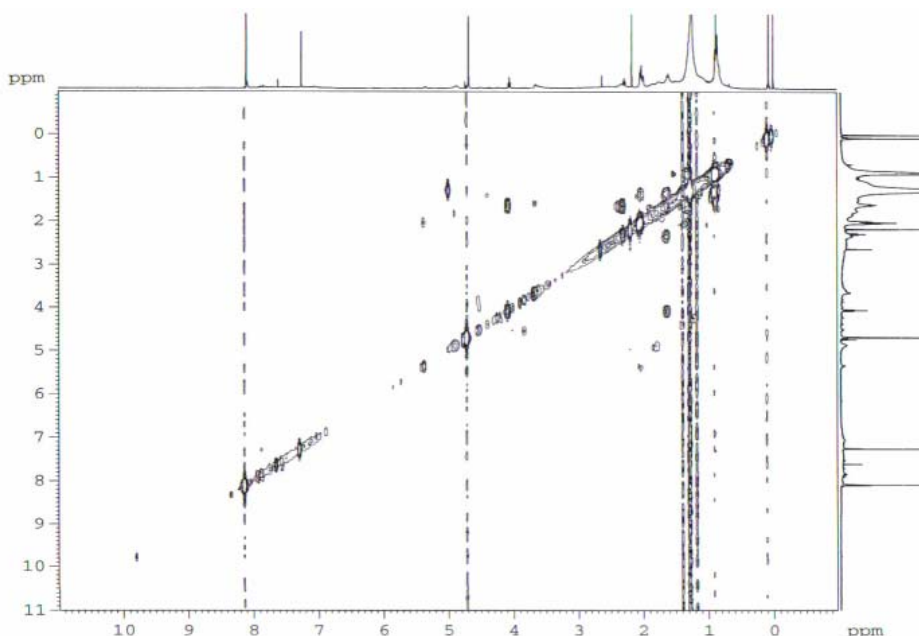


Figure-5. ^1H - ^1H correlation spectroscopy (COSY) spectrum of sample SSA in CDCl_3 run at 400 MHz.

The HSQC spectrum in Figure-6 which is also proton detected gives strong proton-carbon coupling i.e. the protons directly bonded to the carbon. Table-5

summarizes the strong proton-carbon coupling from the HSQC spectrum of Figure-6.

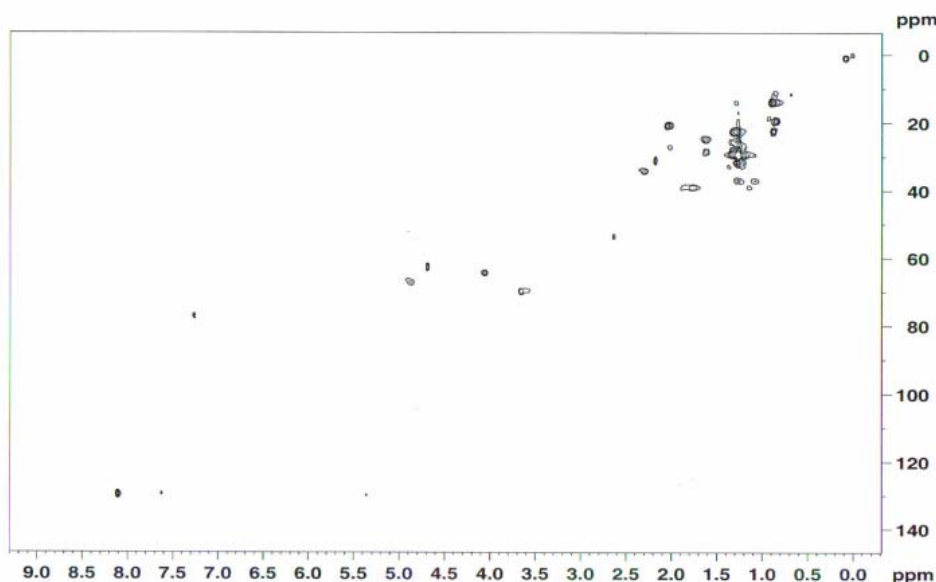


Figure-6. Heteronuclear single quantum correlation (HSQC) spectrum of sample SSA in CDCl_3 (100 MHz for ^1H , 400 MHz for ^{13}C).



Table-5. HSQC correlation data for sample SSAA showing direct proton-carbon correlations as obtained from Figure-6.

¹ H (ppm)	2	2	5.4	8.1	7.6	1.6	1.6	2.3	4.1	2.65
¹³ C (ppm)	21	26	130	130	130	26	28	32	64	54
¹ H (ppm)	2.15	4.9	0.85	0.85	0.85	1.1	1.2	0.7	1.35	1.25
¹³ C (ppm)	31	67	14.1	19.5	22.7	37	37	11.5	17	14

Information obtained from HMBC spectrum in Figure-7 below, capitalizes on weak proton-carbon coupling and suppresses one-bond correlations. A weak

proton-carbon coupling indicates that the proton is two or three bonds away from the carbon. The deduced proton-carbon correlations are summarized in Table-6.

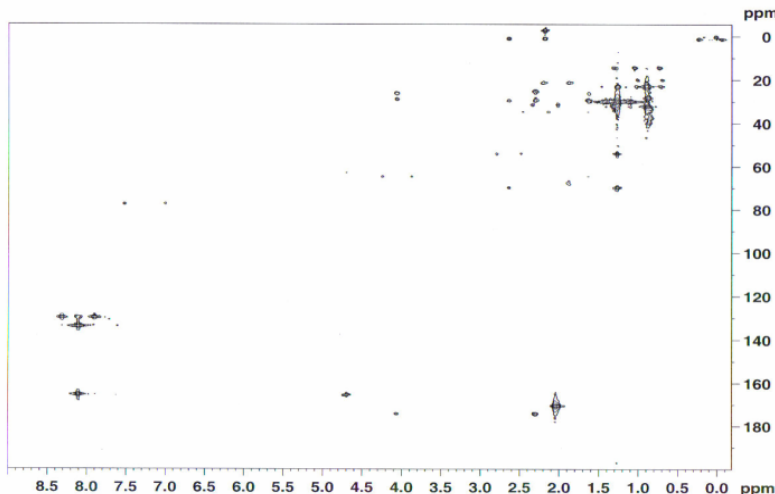


Figure-7. The heteronuclear multiple bond correlation (HMBC) spectrum of sample SSA in CDCl₃ (100 MHz for ¹H, 400 MHz for ¹³C).

Table-6. HMBC correlations data for sample SSA showing proton-carbon multiple bond correlations as obtained from Figure-7.

¹ H (ppm)	4.1	2.3	8.1	8.1	4.1	4.1	2	2	1.6	1.6
¹³ C (ppm)	174	174	134	165	26	28	170	32	26	28
¹ H (ppm)	2.3	0.7	7.9	0.7	0.75	1.05	1.3	1.25	1.25	1.25
¹³ C (ppm)	28	23	130	20	14.1	14.1	14.1	69	54	22
¹ H (ppm)	3.9	2.65	8.3	2.65	2.5	2.8	1.9	2.2	2.7	0.75
¹³ C (ppm)	64	29.5	130	70	54	54	21	21	20	23
¹ H (ppm)	1.05	1.25	0.9	0.9	0.9	2.15	1.45	1.15	2.3	4.2
¹³ C (ppm)	23	23	23	28	33	35	23	23	25	64

DISCUSSIONS

The TLC tests identified 9 different compounds present in the extracts. The TLC results support proton NMR spectrum which shows that the samples are mixtures of different compounds with overlapping and complex peaks.

For air reactivity the elements of most important influence are vanadium, nickel [15], sodium [16], lead and copper [17] whereas for CO₂ reactivity the elements of

most important influence are iron [18], sodium [19] and calcium [20]. The CO₂ reactivity was high in sample SSA (166 mg/g h) due to high levels of Fe, Na, Ca and low in sample SSB (25 mg/g h) due to low concentrations of Na and Ca. The low reactivity value of sample SSB was due to low elemental composition. The coke CO₂ reactivity showed a moderate correlation with Na, Fe and Ca as shown in Figure-8.

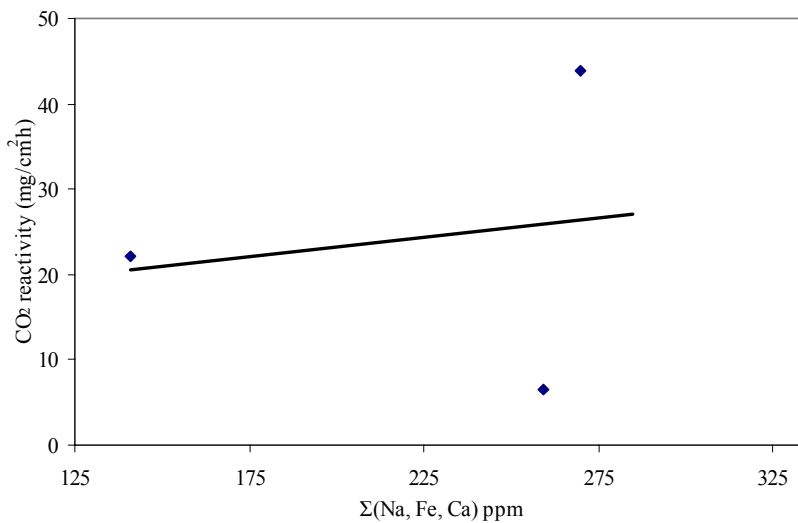


Figure-8. Correlation between CO_2 reactivity and $\Sigma(\text{Na, Fe, Ca})$ content for investigated cokes.

Air reactivity was high in sample SSC (262 mg/g h) and low in sample SSB (39.6 mg/g h). This matched the expected strong correlation with the Vanadium (V) composition of the samples as shown in Figure-9. Sample SSC recorded the expected high air reactivity value due

largely to the high concentration of V (378 ppm), and partially by the concentrations of Na (43 ppm), and Ni (170 ppm). Furthermore, the low air reactivity value for sample SSB was due to the low levels of V (68 ppm), Na (28 ppm) and Ni (44 ppm).

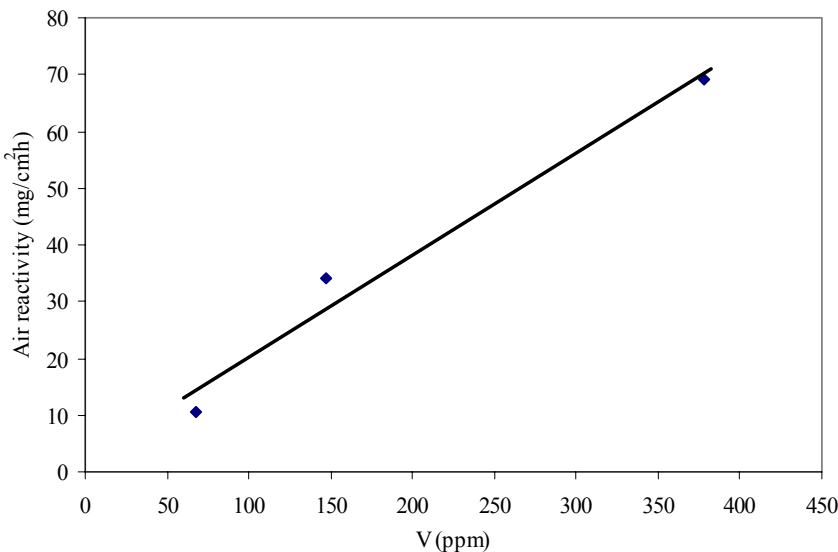


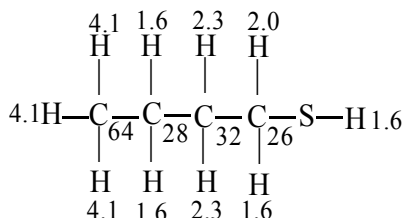
Figure-9. Correlation between air reactivity and V content for investigated cokes.

From Figure-3, the aliphatic sulphur containing functional group of interest may occur at a chemical shift (δ) range of 1.2-1.8 ppm. From Figure-4 the carbon containing the expected functional group of interest falls within the range of δ 5-45 ppm. In Figure-5 the protons at δ 1.6 ppm are coupled to protons at δ 2.3 ppm and δ 4.1 ppm. Sulphhydryl protons can usually exchange at a low rate so that at room temperature they are coupled to protons on adjacent carbon atoms [13]. This phenomenon was observed as the proton chemical shift of 1.6 ppm was directly attached to carbon at 826 ppm as is evident in

Figure-6. Furthermore, the δ 1.6 ppm exhibits a two bond correlation to the δ 26 ppm carbon as in Figure-5 and tabulated in Table-5. This indicates that the suspected organosulphur compound is a thiol with the sulphur atom sandwiched between carbon at 826 ppm and a sulphhydryl proton of δ 1.6. The proton at δ 2.0 ppm is also bonded to carbon at 826.0 ppm. Furthermore, the δ 1.6 ppm exhibits a two bond correlation to the δ 26 ppm carbon as shown in the Figure-5. From Figure-5, the proton δ 4.1 ppm is next to the proton δ 1.6 ppm which in turn is adjacent to proton δ 2.3 ppm. The HSQC data in Figure-6 shows that proton



$\delta_{4.1}$ is directly bonded to carbon at δ_{64} ppm, proton $\delta_{1.6}$ ppm is directly bonded to carbon at δ_{28} ppm, and proton $\delta_{2.3}$ ppm is directly bonded to carbon at δ_{32} ppm. Furthermore, Figure-7 and its corresponding Table-6, shows that carbon at δ_{32} ppm is joined to carbon at δ_{26} ppm by the formation of a three bond correlation between proton $\delta_{1.6}$ ppm and carbon δ_{28} ppm. Proton $\delta_{2.3}$ ppm is linked to carbon at δ_{28} ppm by two bond correlation in Table-6. A two bond correlation is also formed between the proton $\delta_{4.1}$ and carbon at δ_{28} ppm. This identifies the organosulphur as 1-butanediol, $n\text{-C}_4\text{H}_{10}\text{S}$.



CONCLUSIONS

Among the determinant parameters that affect coke reactivity, the elemental composition of the coke remains the single most important parameter. The high V content in the cokes had a significant impact on air reactivity and showed a strong correlation. Air reactivity was highest in sample SSC (262 mg/g h) at a V concentration of 378 ppm and lowest in sample SSB (39.6 mg/g h) at a V concentration of 68 ppm. Coke sample SSA recorded the highest CO_2 reactivity value of 166 mg/g h while coke sample SSB recorded the lowest value of 25 mg/g h. The coke CO_2 reactivity further showed a moderately strong correlation with the combined effects of Na, Fe and Ca concentrations. The compound 1-butanethiol was identified as a possible organosulphur compound responsible for inhibiting the catalytic effect of Na on CO_2 reactivity.

REFERENCES

- [1] Meier M. W. 2006. The impact of raw material quality and anode manufacturing parameters on the behaviour in electrolysis. 25th International Course on Process Metallurgy of Aluminium, Trondheim-Norway, May 29 - June 02. 1: 133-134.
- [2] Meyers R. A. 1986. Handbook of Petroleum Refining Processes. McGraw Hill.
- [3] Perruchoud R. C. 2001. Anode properties cover materials and cell operation. Light Metals. p. 695.
- [4] Fischer W. K. and Perruchoud R.C. 1985. Influence of Coke Calcining Parameters on Petroleum Coke Quality. Light Metals, AIME, New York. p. 811.
- [5] Keller F., Fischer W. K. Consumption of anode carbon during aluminium electrolysis. Light Metals. p. 729.
- [6] Baber A. M., Proulx L. A. 1994. Anode consumption study. Light Metals. p. 677.
- [7] Billehaug K., Øye H. A. 1981. ALUMINIUM 57. p. 146 and p. 228.
- [8] Samanos B., Dreyer C. 2001. Impact of Coke Calcination level and Anode Baking Temperature on Anode Properties. Light Metals. p. 681.
- [9] Rolle G. J. and Czikall A.R. 2001. Use of Coke Air Reactivity Testing for Predicting Anode Air Reactivity. Light Metals. p. 675.
- [10] Foosnæs T. 2007. Private communication. 15 January.
- [11] Maxted E. B. 1951. The poisoning of metallic catalysts. Adv Catal. 3: 129.
- [12] Hume S. M., Fischer W. K., Perruchoud R. C., Metson J. B., Baker R. T. K. 1993. Influence of petroleum coke sulphur content on the sodium sensitivity of carbon anodes. Light Metals. p. 535.
- [13] Silverstein R. M. and Webster F. X. 1998. Spectrometric Identification of Organic Compounds. 6th Ed. NY: Wiley interscience publication. p. 2, 14, 69, 144, 168, 232, 255-264.
- [14] Crews P., Jaspars M., Rodrigue J. 1998. Organic structure analysis. 1st Ed. NY: Oxford University Press. p. 7, 23, 28-32, 230-233.
- [15] Reis T. 1977. Chem. Tech. 7(6): 336.
- [16] Lazarev V. D., Yanko E. A., Zakharov V. V. 1978. Sov. J. Nonferrous Metals. 19(2): 38.
- [17] Sekhar J. A. and Liu J. 1999. Preferential Oxidation Processes of Carbons used in the Hall-Héroult Cell. Light Metals. p. 531.
- [18] Kolodin E. A., Nikitin V. 1982. Ya, Tsvet. Met. (8): 44.
- [19] Wilkening. S. 1994. Why the sulfate reactivity test. Light Metals. p. 643.
- [20] Rey Boero J. F. 1981. Studies on anode reactivity to oxidant gas. Light Metals. p. 441.
- [21] Chmelar J. 2006. Size reduction and specification of granular petrol coke with respect to chemical and physical properties. PhD Thesis. NTNU. p. 15.